Journal of Statistical Physics, Vol. 70, Nos. 5/6, 1993

Field-Dependent Conductivity and Diffusion in a Two-Dimensional Lorentz Gas

András Baranyai,[1,2] Denis J. Evans,[1] and E. G. D. Cohen[3]

Received January 31, 1992; final July 7, 1992

The conductivity and diffusion of a color-charged two-dimensional thermostatted Lorentz gas in a color field is studied by a variety of methods. In this gas, point particles move through a regular triangular array of soft scatterers, where, in the presence of a field, a nonequilibrium stationary state is reached by coupling to a Gaussian thermostat. The zero-field conductivity and diffusion coefficient are computed with equilibrium molecular dynamics dynamics from the Green–Kubo formula and the Einstein relation. Their values are consistent and approach those obtained by Machta and Zwanzig in the limit of hard (disk) scatterers. The field-dependent conductivity is obtained from its constitutive relation, from the coupling constant to the thermostat, and by using the recently derived conjugate pairing rule of Evans, Cohen, and Morriss, from the two maximal Lyapunov exponents of the Lorentz gas in the stationary state. All these methods give consistent results. Finally, elements of the field-dependent diffusion tensor have been computed. At zero field, they are consistent with the zero-field conductivity, but they vanish beyond a critical field strength, suggesting a dynamical phase transition at the critical field; the conductivity appears to remain finite, approaching a constant value for large field strengths.

KEY WORDS: Conductivity, diffusion, field-dependence, Lorentz gas, Lyapunov exponents.

1. INTRODUCTION

The two-dimensional Lorentz gas we consider was studied before[1,2] and consists of a two-dimensional triangular lattice of hard-disk scatterers

[1] Research School of Chemistry, Australian National University, GPO Box 4, Canberra, ACT 2601, Australia.

[2] Permanent address: Laboratory of Theoretical Chemistry, Eötvos University, Budapest Múzeum krt 6-8, 1088 Hungary.

[3] Rockefeller University, New York, New York 10021.

0022-4715/93/0300-1085$07.00/0

through which point particles move, which collide with the scatterers. If a is the radius of the disks and r the distance between the centers of nearest neighbor disks, $w = r - 2a$ is the gap through which the particles must move to transfer from one triangular region to another. (See Fig. 1). There is a limit density of the scatterers above which we study the model: if $r \leqslant 4a/\sqrt{3}$, then there is no way for the particles to travel freely through the gaps without colliding with the scatterers. As will be explained below, we replaced the hard-disk scatterers by scatterers which interact with the point particles through a continuous potential.

In the usual Lorentz gas the lattice is infinite and the moving point particles are independent. Here we study the motion of a set of particles moving under the influence of an external field $\mathbf{F}_c$ through the scatterers. To enable the formation of a steady state (ss), we thermostat the system of moving particles. This thermostat is chosen such that the total kinetic energy of the set of moving particles, measured with respect to their instantaneous average velocity, i.e., the peculiar kinetic energy K, is a constant of the motion.

In order to simulate a nonequilibrium steady state, we employ the equations of motion for the nonequilibrium molecular dynamics (NEMD) color conductivity algorithm[3]:

$$\begin{aligned} \dot{\mathbf{q}}_i &= \frac{\mathbf{p}_i}{m_i} \\ \dot{\mathbf{p}}_i &= \mathbf{F}_i + \mathbf{i}c_i F_c - \alpha(\mathbf{p}_i - \mathbf{i}m_i c_i J_x) \end{aligned} \tag{1}$$

Here $\mathbf{q}_i$, $\mathbf{p}_i$, and m_i are the position, momentum, and mass of the moving particle i, respectively. Furthermore, $m_i = m$ for all $i \equiv 1,..., N$, and $\mathbf{F}_i$ is the

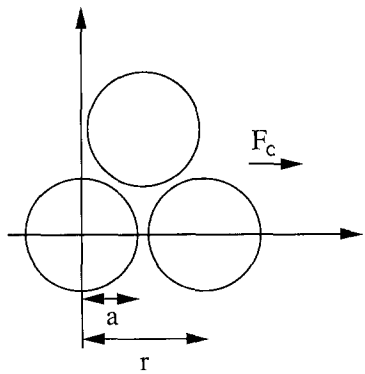

Fig. 1. Geometry of the scatterers with radius a and distance r and applied color field $\mathbf{F}_c$ in the x direction.

Newtonian force on particle i, representing the interaction between this particle and the fixed scatterers. In order to study the conductivity of the set of moving particles, the particles are "charged" with a color, $c_i = (-1)^i$ ($= +1$ or 1), which couples, like an electric charge, to an external field; here the color field $\mathbf{F}_c = \mathbf{i} F_c$, where $\mathbf{i}$ is a unit vector in the x direction and $F_c = |\mathbf{F}_c|$ is the strength of the field. A difference with the electric case is that, in the absence of the external field, the system is color-blind, i.e., all particles behave identically, since for $\mathbf{F}_c = \mathbf{0}$, there is no way of distinguishing the (color) charge of the particles. Moreover, the color conductivity system does not have the complications inherent in the long-range Coulombic interactions of the corresponding electrical conductivity problem. In our calculations the color field $\mathbf{F}_c$ acts homogeneously in the x direction (see Fig. 1), so that J_x, the instantaneous value of the current $\mathbf{J} = \mathbf{i} J_x$ per particle generated by $\mathbf{F}_c$, is

$$J_x = \frac{1}{N} \sum_{i=1}^{N} c_i \frac{p_{ix}}{m} \tag{2}$$

and the color conductivity is defined from the constitutive relation

$$L(F_c) \equiv \frac{\langle J_x \rangle_{ss}}{F_c} \tag{3}$$

where $\langle \cdots \rangle_{ss}$ denotes a steady-state ensemble average. The term involving α in Eq. (1) represents the thermostatting mechanism, where the coupling constant α is the Gaussian thermostatting (Lagrange) multiplier,[3] which is determined by fixing the peculiar kinetic energy of the N moving particles in the system. The peculiar kinetic energy is defined as

$$K = \sum_{i=1}^{N} (\mathbf{p}_i - \mathbf{i} m c_i J_x)^2 / 2m \tag{4}$$

where $\mathbf{p}_i - \mathbf{i} m c_i J_x$ is the peculiar momentum of particle i, since $c_i J_x$ is the instantaneous average velocity of all particles with the same charge as particle i. From (1), (2), and (4), α can be determined to be

$$\alpha = \frac{\sum \mathbf{F}_i \cdot (\mathbf{p}_i - \mathbf{i} c_i m J_x)}{\sum \mathbf{p}_i \cdot (\mathbf{p}_i - \mathbf{i} c_i m J_x)} \tag{5}$$

An effect of the thermostat is that it introduces a coupling between the otherwise independent particles, since it fixes the total peculiar kinetic energy of the particles. In this sense our thermostatted Lorentz gas differs

from the usual Lorentz gas, where particles move strictly independently of each other, so that the N- and the single-particle problems are identical there.

1.1. Linear Case

The zero-field color conductivity $L(0^+)$ is related to the zero-field self-diffusion coefficent $D(0) \equiv D$ of the system by[3]

$$\lim_{F_c \to 0^+} k_B T L(F_c) \equiv k_B T L(0^+) = \lim_{F_c \to 0^+} \frac{k_B T \langle J_x \rangle_{ss}}{F_c} = D \tag{6}$$

Thus the zero-field conductivity can be computed directly by extrapolating the measured current-to-field ratio to field zero. On the other hand, the diffusion coefficient D can be calculated from equilibrium molecular dynamics either by using the Green–Kubo (GK) formula in terms of the velocity autocorrelation function (VCF),

$$D_{GK} = \frac{1}{2} \int_0^\infty dt \left\langle \frac{\mathbf{p}_i(t)}{m} \cdot \frac{\mathbf{p}_i(0)}{m} \right\rangle_{eq} \tag{7}$$

or the Einstein relation (E),

$$D_E = \lim_{t \to \infty} \frac{1}{4t} \langle \Delta \mathbf{q}_i(t) \cdot \Delta \mathbf{q}_i(t) \rangle_{eq} \tag{8}$$

where $\Delta \mathbf{q}_i(t) \equiv \mathbf{q}_i(t) - \mathbf{q}_i(0)$ and $\langle \cdots \rangle_{eq}$ denotes an equilibrium ensemble average. At zero field the diffusion tensor for the Lorentz gas is isotropic, characterized by the scalar D only. For nonzero values of the color field, the diffusion and the conductivity are both anisotropic tensors.

1.2. Nonlinear Case

At nonzero field the conductivity can be determined either directly from the measured current-to-field ratio, as stated in Eq. (3), or from a recently discovered relation between transport coefficients and Lyapunov exponents.[4]

The $4N$ Lyapunov exponents $\{\lambda_i\}$, $i = 1,..., 4N$, measure the exponential (long-time) rates of expansion and contraction of $4N$ lengths associated with the $4N$-dimensional hypercube which characterizes the system in its phase space. The largest Lyapunov exponent characterizes the fastest growing length, the second largest is deduced from the fastest growing area, etc.

There is a simple relation between the sum of all the Lyapunov exponents $\sum_{i=1}^{4N} \lambda_i$ and the average energy removed per unit time by the thermostat $-2K\langle\alpha\rangle_{ss}$. Since in a steady state the average internal energy is constant, $2K\langle\alpha\rangle_{ss}$ must equal the average work performed per unit time on the system by the external color field, i.e., $N\langle J_x(F_c)\rangle_{ss} F_c = NL(F_c)F_c^2$. Using that $K = Nk_B T$, this implies that[4]

$$L(F_c) = -\frac{k_B T}{NF_c^2} \sum_{i=1}^{4N} \lambda_i(F_c) \tag{9}$$

where $\lambda_i(F_c)$ is the ith field-dependent Lyapunov exponent. Although exact, this relation is not very useful. It is exceedingly difficult to calculate the full spectrum of all the $4N$ Lyapunov exponents for systems with more than just a few particles. However, for Hamiltonian systems coupled to a thermostat an essential simplification is possible.[4] For, if one defines conjugate pairs of exponents by grouping the largest and the smallest exponents, the second largest with the second smallest, etc., together, the sum of each such conjugate pair of exponents, $\lambda_i + \lambda_{i'}$, is constant, independent of i. This was called the conjugate pairing rule.[4] Using this rule, one can greatly simplify Eq. (9) and the color conductivity can be written as the sum of the two maximal Lyapunov exponents

$$L(F_c) = -\frac{2k_B T}{F_c^2} [\lambda_{max}(F_c) + \lambda_{min}(F_c)] \tag{10}$$

The pair of maximum and minimum Lyapunov exponents was chosen, since it is the easiest to calculate.[4] In order to obtain the maximal Lyapunov exponents from NEMD simulations, we moved the phases of the particles of the system forward in time simultaneously on two initially close trajectories. The starting point of the second trajectory was created from the starting point of the first one by very slightly perturbing the initial phase space vector $\Gamma(0) \equiv (\mathbf{q}_1, ..., \mathbf{q}_N, \mathbf{p}_1, ..., \mathbf{p}_N)$. We then monitored the growth in the separation distance $d(t)$ between these two phase space trajectories, $d(t) \equiv |\Gamma(t) - \Gamma(0)|$. At long times, the logarithm of this distance is a linear function of time with a slope equal to the largest positive Lyapunov exponent λ_{max} of the system. The smallest (i.e., the most negative) Lyapunov exponent λ_{min} can be calculated by reversing the direction of time and calculating the largest Lyapunov exponent of the ensuing anti-steady state.[4]

Although the conductivity $L(0^+)$ and the diffusion coefficient $D = D(0)$ are directly related in the linear case, this is not so in the nonlinear case. Therefore in the latter case we have to discuss the two

separately. We first discuss the diffusion (tensor) for the nonequilibrium steady state. Away from equilibrium ($F_c \neq 0$), the Lorentz gas becomes anisotropic and the macroscopic convective diffusion equation for the probability density $P_i(\mathbf{r}, t)$ to find particle i at $\mathbf{r}$ at t, given it is at $\mathbf{r} = \mathbf{0}$ at $t = 0$, reads

$$\frac{\partial P_i(\mathbf{r}, t)}{\partial t} + \mathrm{i}c_i \langle J_x \rangle \cdot \frac{\partial P_i(\mathbf{r}, t)}{\partial \mathbf{r}} = -\frac{\partial}{\partial \mathbf{r}} \cdot \mathbf{D} \cdot \frac{\partial}{\partial \mathbf{r}} P_i(\mathbf{r}, t) \tag{11}$$

where $\mathbf{D} = \mathbf{D}(F_c)$ is the field-dependent diffusion tensor. In the linear case, $\mathbf{D}(0) = D\mathbf{1}$, where $\mathbf{1}$ is the unit tensor.

As shown on ref. 6, the symmetrized diffusion tensor has a simple Einstein relation of the form

$$\mathbf{D}(F_c) = \lim_{t \to \infty} \frac{1}{4t} \langle \Delta \hat{\mathbf{q}}_i(t) \, \Delta \hat{\mathbf{q}}_i(t) \rangle_{\mathrm{ss}} \tag{12}$$

where

$$\begin{aligned} \Delta \hat{\mathbf{q}}_i(t) &\equiv \Delta \mathbf{q}_i(t) - \langle \Delta \mathbf{q}_i(t) \rangle_{\mathrm{ss}} \\ &= \mathbf{q}_i(t) - \mathbf{q}_i(0) - \mathrm{i}c_i \langle J_x \rangle_{\mathrm{ss}} t \end{aligned} \tag{13}$$

We remark that $\Delta \hat{\mathbf{q}}_i(t)$ is the displacement of particle i in time t relative to the average (drift) velocity $c_i \langle J_x \rangle_{\mathrm{ss}}$.

2. MODEL

Although most versions of the Lorentz gas employ hard interactions between the moving particles and the scatterers,[7] we do not do this. Our reasons are twofold. First, there is no explicit analytical solution for the motion of a hard particle under the combined influence of an external color field and a Gaussian thermostat. Second, the measurement of the Lyapunov exponents for systems of hard particles is very difficult.

For, while between collisions the phase space separation varies continuously as a nonexponential function of the time, at the instant of collision, jumps occur in the phase space separation of the two neighboring phase space trajectories. For these hard-core models this complicates the determination of the Lyapunov exponents for two reasons. (1) The computer dynamics has to switch all the time from continuous (between collisions) to discontinuous (at collisions) techniques; and (2) the Lyapunov exponents have to be determined by long-time averaging over many jumps. This is especially cumbersome for the determination of the smallest

Lyapunov exponent, since that exponent must be determined before inaccuracies in the time-reversed trajectory become comparable with typical interparticle spacings or relative velocities and the anti-steady state decays to a steady state again.[4]

We therefore used a continuous potential to describe the interactions between particles and scatterers, based on a Weeks–Chandler–Anderson (WCA)-like potential, which contains a hard-disk potential as a limit and is defined[7]

$$\begin{aligned}
\phi(R) &= \infty && \text{for} \quad R \leqslant a \\
&= 4\varepsilon\left[\left(\frac{\sigma}{R-a}\right)^{12} - \left(\frac{\sigma}{R-a}\right)^{6}\right] + \varepsilon && \text{for} \quad a < R \leqslant a + 2^{1/6}\sigma \\
&= 0 && \text{for} \quad R > a + 2^{1/6}\sigma
\end{aligned} \tag{14}$$

where R is the distance between the center of the scatterer and the pointlike moving particle. For all values of σ and ε, $\phi(R)$ is continuous. In the limit of vanishing σ or ε, our potential reduces to the hard-disk (HD) interaction

$$\lim_{\sigma \to 0} \phi(R) = \lim_{\varepsilon \to 0} \phi(R) = \phi_{\mathrm{HD}}(R) \tag{15}$$

where

$$\begin{aligned}
\phi_{\mathrm{HD}}(R) &= \infty \qquad \text{for} \quad R < a \\
&= 0 \qquad \text{for} \quad R > a
\end{aligned} \tag{16}$$

We note that the modified WCA potential used in Eq. (14) is considerably steeper than the original one, so that the determination of the Lyapunov exponents is not as accurate, especially at low field strengths.

We studied a system of 484 moving particles. All results are given in dimensionless form using the hard-disk radius a, the mass of the moving particle m, and the mean square peculiar velocity of the moving particles, $\overline{v^2} = \langle (\mathbf{p}_i - \mathbf{i}mc_i J_x)^2/2m \rangle_{\mathrm{ss}}$, to define our units of length, mass, and time, respectively. Because of the thermostatting of the system, $\overline{v^2}$ is constant.

For all simulations $m\overline{v^2}/\varepsilon$ was set equal to 4×10^4. Using that $m\overline{v^2} = 2k_{\mathrm{B}}T$, this corresponds to a reduced Lennard-Jones temperature $T^* = k_{\mathrm{B}}T/\varepsilon$ of 2×10^4, for which the scatterers behave quite like hard disks. Furthermore, we used values of σ/a in the range 1–0.1, and, of course, the hard-disk limit is approached for $\sigma/a \to 0$.

The reduced time step $(\Delta t)(\overline{v^2})^{1/2}/a$ varied from 0.003 to 0.00004, depending on σ. As one approaches the hard-disk limit, the required timestep goes to zero, so that the calculations become more and more

lengthy. In computing averages, we used that at equilibrium the diffusion tensor for the system is isotropic (i.e., $D_{xx} = D_{yy} = D$, $D_{xy} = D_{yx} = 0$). Errors can be estimated from the differences between the Green–Kubo (D_{GK}) and the Einstein (D_E) diffusion coefficients.

3. RESULTS

The results of the equilibrium calculations are shown in Table I. The last column of the table shows the reduced mean internal energy per particle $e^* \equiv e/(m\overline{v^2})$; since $e^* = 0.5$ in the hard-disk limit, we can use the tabulated values of e^* to indicate how close the system is to the hard-disk limit. We see that the differences between D^*_{GK} and D^*_E are at most about 3%.

If we extrapolate D to the $\sigma = 0$ (hard-disk) limit, our results are in good agreement with the calculations of Machta and Zwanzig[1] for hard disks. In fact, our results for $w = 0.1a$ are $D = 0.0985 \pm 0.005$; for $w = 0.2a$, $D = 0.167 \pm 0.01$; and for $w = 0.3a$, $D = 0.247 \pm 0.008$, while the corresponding Machta–Zwanzig simulation value are 0.100 ± 0.01, 0.18 ± 0.01, and 0.250 ± 0.01, respectively.

It is interesting to compare the VCFs of the two models for different

Table I. Equilibrium Results[a]

w^*	σ^*	D^*_{GK}	D^*_E	ε^*
0.3	1.0	0.148	0.147	0.5129
0.3	0.5	0.199	0.196	0.5056
0.3	0.4	0.209	0.207	0.5043
0.3	0.3	0.220	0.217	0.5032
0.3	0.2	0.226	0.225	0.5021
0.2	0.7	0.111	0.109	0.5028
0.2	0.6	0.120	0.119	0.5099
0.2	0.5	0.132	0.133	0.5081
0.2	0.4	0.141	0.141	0.5062
0.2	0.3	0.149	0.146	0.5045
0.2	0.2	0.148	0.146	0.5028
0.2	0.1	0.157	0.152	0.5014
0.1	0.4	0.064	0.066	0.5104
0.1	0.3	0.076	0.075	0.5073
0.1	0.2	0.082	0.081	0.5046
0.1	0.1	0.091	0.090	0.5021

[a] $w^* = w/a$, $\sigma^* = \sigma/a$, $D^*_{GK} = D_{GK}/a(\overline{v^2})^{1/2}$, $D^*_E = D_E/a(\overline{v^2})^{1/2}$, and $e^* = e/m\overline{v^2}$, where D_{GK} is the Green–Kubo diffusion coefficient evaluated using Eq. (7) and D_E is the Einstein diffusion coefficient evaluated using Eq. (8).

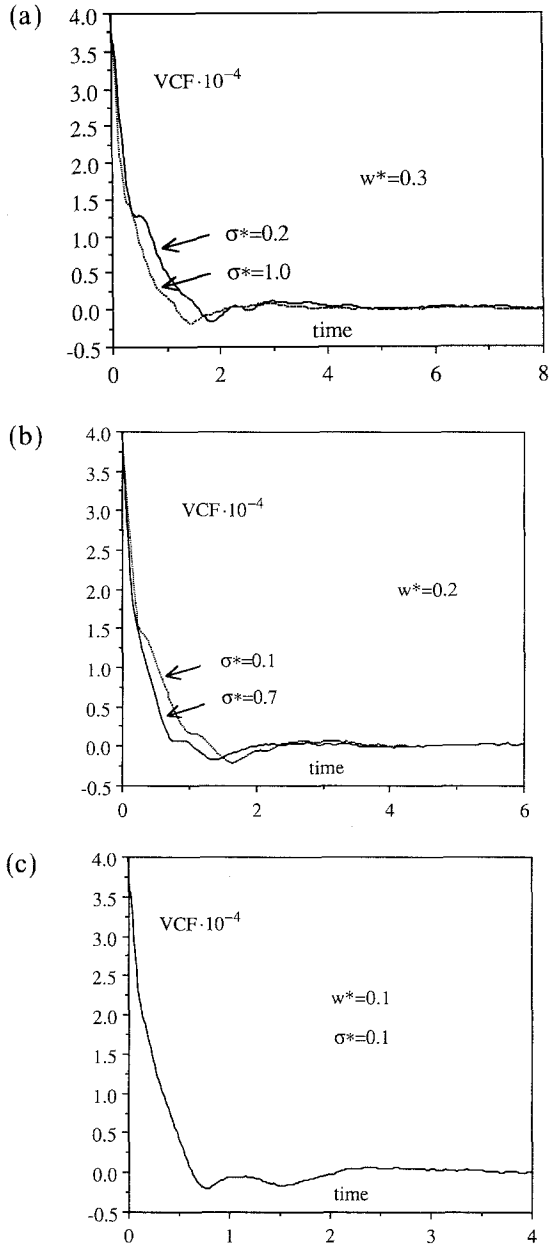

Fig. 2. The reduced equilibrium velocity autocorrelation function $\mathrm{VCT}^* = \langle \mathbf{v}(0) \cdot \mathbf{v}(t^*) \rangle_{\mathrm{eq}} / \overline{v^2}$ as a function of reduced time $t^* = t(\overline{v^2})^{1/2}/a$ for $w^* = w/a =$ (a) 0.3, (b) 0.2, (c) 0.1, and various values of $\sigma^* = \sigma/a$.

Table II. Results of NEMD Simulations for $w^* = 0.3$, $\sigma^* = 1.0$[a]

F_c^*	L_d^*	L^*_{th}	L_L^*	D_{xx}^*/T^*	D_{yy}^*/T^*	e^*
0.0				0.294	0.294	0.5129
0.25	0.286	0.286		0.216	0.278	0.5130
0.75	0.279	0.,278		0.108	0.280	0.5140
1.25	0.288	0.288	0.346	0.118	0.098	0.5150
1.50	0.361	0.360	0.374	0.082	~0 [0.134]	0.5155
1.75	0.403	0.403	0.400	0.044	~0 [0.110]	0.5165
2.00	0.439	0.439	0.444	0.034	~0 [0.107]	0.5173
2.25	0.493	0.493	0.514	0.038	~0 [0.064]	0.5190
2.50	0.470	0.470	0.478	0.032	~0 [0.053]	0.5210
2.75	0.435	0.434	0.450			0.5230
3.125	0.389	0.389	0.380	0.006	~0 [0.037]	0.5248
3.75	0.361	0.361	0.352	~0 [0.10]	~0 [0.029]	0.5293

[a] $L_d^* = L_d m(\overline{v^2})^{1/2}/c_1^2 a$, $L^*_{\text{th}} = L_{\text{th}} m(\overline{v^2})^{1/2}/c_1^2 a$, $L_L^* = L_L m(\overline{v^2})^{1/2}/c_1^2 a$, and $D_{\alpha\alpha}^*/T^* = D_{\alpha\alpha} m(\overline{v^2})^{1/2}/k_B T a$ are given as a function of $F_c^* = F_c a/m\overline{v^2}$ ($\alpha = x$ or y and $c_1^2 = 1$). The entries ~0 for $D_{\alpha\alpha}^*/T^*$ denote consistency with a value zero; for these cases we give the reduced mean square displacements (see text) in square brackets.

w and σ values (see Fig. 2). For small σ values our results are again very close to the hard-disk results of Machta and Zwanzig.[1]

A difference between the equilibrium and nonequilibrium simulations is that for finite values of the color field, not only the diffusion, but also the conductivity, is not isotropic. We have made no attempt, though, to explore systematically the finite field anistropy of the conductivity of the model; our conductivity L is always in the field direction, so that in the anisotropic case, $L = L_{xx}$, where L_{xx} is the xx element of the conductivity tensor.

In Tables II and III we show the results of our finite-field NEMD

Table III. Tesults of NEMD Simulations for $w^* = 0.2$ and $\sigma^* = 0.7$[a]

F_c^*	L_d^*	L^*_{th}	L_L^*	D_{xx}^*/T^*	D_{yy}^*/T^*	e^*
0.0				0.217	0.217	0.5028
0.25	0.205	0.204		0.164	0.200	0.5120
0.75	0.193	0.192		0.086	0.214	0.5125
1.50	0.210	0.208	0.244	0.081	0.114	0.5135
2.00	0.266	0.266	0.252	0.054	0.004	0.5150
2.50	0.371	0.374	0.376	0.006	~0 [0.048]	0.5193
3.00	0.381	0.381	0.386	~0 [0.119]	~0 [0.032]	0.5213
3.50	0.364	0.354	0.354	~0 [0.008]	~0 [0.026]	0.5245

[a] See Table II for notation.

calculations. They show, in reduced form, the color conductivity as measured by a nonequilibrium average of the color current L_d, by the value of the thermostatting multiplier $L_{\text{th}} = 2k_B T\langle\alpha\rangle_{ss}/F_c^2$, and by calculating the maximal Lyapunov exponents using the conjugate pairing rule, L_L, respectively.

The errors in the Lyapunov exponents were approximately $\pm 4\%$ but at least 0.004, which means that we could not get meaningful results for the smallest field values. The accuracy of the L_d values is $\pm 3\%$ at very low fields and $\pm 1\%$ at higher fields. The agreement between L_d and L_{th} is a good check of the correctness of the computer program. The values of L obtained by the three different methods are in statistical agreement except at the lowest values of the color field, where L_L differs from L_d and L_{th} by approximately two standard deviations. The rather large deviations of L_L^* from $L_d^* \approx L_{\text{th}}^*$ are mainly due to the fact that the WCA potential we used is still close to a hard-disk potential and therefore too steep to yield accurate values of L_L^*. Our results here are therefore not as good as those obtained before for the maximal Lyapunov exponents associated with the viscosity of a WCA fluid.[4] In addition to the conductivity L, we also determined numerically the xx and yy elements of the diffusion tensor using Eq. (12). For ease of comparison, columns 5 and 6 use the same units as that of the corresponding L values, so that in the zero-color-field limit

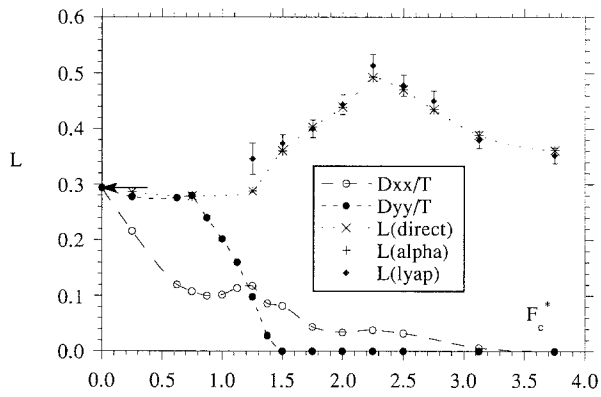

Fig. 3. Reduced field-dependent conductivity L^* (see Table II) as a function of the reduced applied color field strength F_c^*. Five different computational methods are compared: (1) direct NEMD, i.e., averaging of the steady-state flux (direct, L_d^*, (2) NEMD averaging of the thermostatting multiplier L_{th}^*, (3) using the conjugate pairing rule ($L_{L_{\text{yap}}}^*$) and (4, 5) two equilibrium methods, which give $L(0^+)$ only: Green–Kubo and Einstein; they are indistinguishable on the scale of this graph. The state point is $w^* = 0.3$, $\sigma^* = 1$. We also show the reduced elements of the field-dependent diffusion tensor $D_{\alpha\alpha}^*/T^*$ ($\alpha = x, y$) (see Table II) as a function of F_c^*. At zero field, $D_{xx}^*/T^* = D_{yy}^*/T^*/T^* = L^*(0^+)$.

we should see that $L^* = D^*_{\alpha\alpha}/T^*$ for $\alpha = x$ or y. That this is indeed so can be seen in Fig. 3, where the limiting zero-field results computed using the Green–Kubo and the Einstein expressions are shown by the arrow. The values in Table II are plotted in Fig. 3.

4. DISCUSSION

1. We have computed the conductivity and the diffusion tensor for a Lorentz gas as a function of the applied (color) field. For all values of the color field the conductivity obtained directly from computer simulations agrees, within statistical uncertainties, with the values of the conductivity computed using theoretical expressions, in particular the conjugate pairing rule of Eq. (10).

It is interesting to note that while in the zero-field limit $L^*(0^+) = D^*_{\alpha\alpha}/T^*$ for $\alpha = x$ or y, at finite values of the color field the behavior of the conductivity and the elements of the diffusion tensor are completely different. In fact there is then no simple Einstein-like relation between the conductivity (tensor) and the diffusion (tensor). While the conductivity is a nonmonotonic function of the field strength, which exhibits a maximum at $F_c^* \cong 2.25$ and appears to approach a constant for our largest values of $F_c^* \approx 3.75$, D_{xx} and D_{yy} appear to approach zero before this limit. Thus, while the conductivity remains finite, the diffusion tensor goes to zero with increasing field.

The very quick decrease of the elements of the diffusion tensor to zero is perhaps an indication of a field-induced (dynamical) phase transition in the diffusive behavior of the system, while the conductivity remains continuous, only showing a maximum. Thus, with the peculiar kinetic energy remaining constant, the diffusive motion of the particles relative to their average (drift) velocity seems to disappear rather quickly at finite field values. In fact, not only do the $D_{\alpha\alpha}$ vanish, i.e., the mean square displacements grow slower than t, the mean square displacements $2D_{\alpha\alpha}t$ themselves eventually vanish as well. For that reason, we have indicated for those entries in the Tables II and III where the diffusion tensor is indistinguishable from zero also the corresponding reduced mean square displacements $\langle \Delta\hat{q}_\alpha(t)\, \Delta\hat{q}_\alpha(t) \rangle_{ss}/a^2$ in square brackets. Physically, the color-charged particles move with increasing color field with an increasing average (drift) velocity through the scatterers in the direction of the field, while the mean square displacements (measured relative to this drift velocity) decrease, at first, less fast than linear with time, then, after the elements of the diffusion tensor have vanished, they drop to zero. Of the elements of the diffusion tensor, D_{yy} perpendicular to the colot field vanishes first at a reduced color field value of $F_c^* \approx 1.5$, after which D_{xx},

parallel to the color field, vanishes at a reduced field of $F_c^* \approx 3.2$. In a Lagrangian coordinate frame moving with the particles, the motion of the particles becomes therefore, with increasing color field strength, increasingly constrained to the direction of the color field.

2. The disappearance of diffusion in the Lorentz model at high fields is interesting since it might serve as a model for electrophoresis, where chemical mixtures in a gel, for instance, are separated under the combined influence of an electric field and diffusion. Here the diffusion counteracts the separation of the species in the mixture, which occurs as a result of the different conductivities (mobilities) of the species. Our Lorentz model, in which the gel is replaced by fixed scatterers, suggests that the diffusion could perhaps be reduced significantly at high fields, leading then in principle to improved separation rates of the mixture species.

3. In Fig. 4 we have sketched the mean square displacements of the $y \equiv q_y$ component of a particle i relative to the drift velocity [cf. Eq. (13)] as a function of time for a number of field strengths F_c. They are remarkably like those of a solid. For, while the short-time linear rise is common to liquids and solids, the longer-time behaviors of liquids and solids differ: for liquids this linear behavior continues, while for solids it changes to damped oscilations around the time-averaged mean square displacements about a lattice site. The same happens in our Lorentz model. It seems to imply that while in the solid it is the atoms that vibrate around their fixed lattice sites, here it is the point particles that carry out a *vibrating* motion with respect to the disks, when viewed from a comoving Lagrangian cooordinate system.

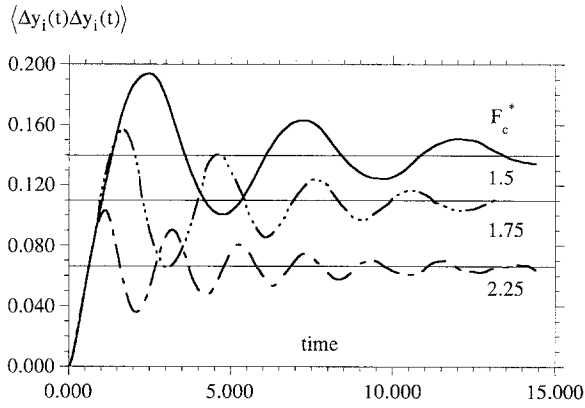

Fig. 4. Averages of the mean square displacement in the y direction relative to the drift velocity as a function of t^* for three values of the reduced color field F_c^* for which D_{yy} is zero. The state point is $w^* = 0.3$, $\sigma^* = 1$.

4. We emphasize that although we carried out a number of investigations in the nonlinear regime as a function of increasing field strength, the behavior in this regime turned out to be so complicated that only a beginning of a study of the nonlinear regime can be considered to have been made.

REFERENCES

1. J. Machta and R. Zwanzig, *Phys. Rev. Lett.* **50**:1959 (1983).
2. P. Gaspard and G. Nicolis, *Phys. Rev. Lett.* **65**:1693 (1990); see also P. Gaspard and S. A. Rice, *J. Chem. Phys.* **90**:2225, 2242, 2555 (1989).
3. D. J. Evans and G. P. Morriss, *Statistical Mechanics of Nonequilibrium Liquids* (Academic Press, London, 1990).
4. D. J. Evans, E. G. D. Cohen, and G. P. Morris, *Phys. Rev. A* **42**:5990 (1990).
5. D. J. Evans, *Phys. Rev. A* **44**:3630 (1991); S. Sarman, D. J. Evans, and P. T. Cummings, *J. Chem. Phys.* **95**:8675 (1991).
6. B. Moran, W. G. Hoover,..., *J. Stat. Phys.* **48**:709 (1987).
7. J. D. Weeks, D. Chandler, and H. C. Andersen, *J. Chem. Phys.* **54**:5237 (1971).